Journal of the Korean Chemical Society
2024, *Vol. 68, No. 3*
Printed in the Republic of Korea
https://doi.org/10.5012/jkcs.2024.68.3.139

Acid-Catalyzed Hydrolysis of Hexacyanoferrate (III) to Prussian Blue *via* Sequential Mechanism

Youngjin Jeon

Department of Applied Chemistry, College of Science and Technology, Konkuk University, 268 Chunwondaero Chungju 27478, Korea.
E-mail: jeonyj@kku.ac.kr

(Received March 12, 2024; Accepted April 14, 2024)

ABSTRACT. This study aims to elucidate the mechanism involved in the hydrolysis of the hexacyanoferrate(III) complex ion ($Fe(CN)_6^{3-}$) and the mechanism leading to the formation of Prussian blue ($Fe^{III}_4[Fe_{II}(CN)_6]_3 \cdot xH_2O$, PB) in acidic aqueous solutions at moderately elevated temperatures. Hydrolysis constitutes a crucial step in generating PB through the widely used single-source or precursor method. Recent PB syntheses predominantly rely on the single-source method, where hexacyanoferrate(II/III) is the exclusive reactant, as opposed to the co-precipitation method employing bare metal ions and hexacyanometalate ions. Despite the widespread adoption of the single-source method, mechanistic exploration remains largely unexplored and speculative. Utilizing UV-vis spectrophotometry, negative-ion mode liquid chromatography-electrospray ionization-mass spectrometry (LC-ESI-MS), and a devised reaction, this study identifies crucial intermediates, including aqueous $Fe^{2+/3+}$ ions and hydrocyanic acid (HCN) in the solution. These two intermediates eventually combine to form thermodynamically stable PB. The findings presented in this research significantly contribute to understanding the fundamental mechanism underlying the acid-catalyzed hydrolysis of the hexacyanoferrate(III) complex ion and the subsequent formation of PB, as proposed in the sequential mechanism introduced herein. This finding might contribute to the cost-effective synthesis of PB by incorporating diverse metal ions and potassium cyanide.

Key words: Hexacyanoferrate, Acid-catalyzed hydrolysis, Prussian blue, Mechanism study, ESI mass spectra

INTRODUCTION

Prussian blue (PB), the first coordination polymer, boasts a historical legacy spanning over 300 years, primarily in applications such as a pigment for painting and dyeing clothes.[1] PB and its analogs, commonly referred to as Prussian blue analogs (PBAs), have garnered attention across diverse fields, including electrochromic sensors,[2] radioactive metal removal,[3] molecular magnets,[4] CO_2 and SO_2 absorption,[5] hydrogen storage,[6] catalysts for H_2O_2 reduction,[7] and as electrode materials in lithium-ion or sodium-ion batteries (LIBs and SIBs) and supercapacitors.[8] The synthesis of PB and PBAs has traditionally involved two main approaches.[9] The first is the co-precipitation method, which combines metal ions and hexacyanometalate complex ions to form PBAs, enabling the synthesis of various bimetallic or multimetallic PBAs.[5b,10] The second method is the single-source approach, utilizing a hexacyanometalate ion as the sole reactant for nanocrystalline PB and PBAs in acidic aqueous solutions and elevated temperatures, often under hydrothermal conditions.[11] The single-source method can be extended to domain-separated bimetallic PBAs through the dual-source method.[12]

Focusing on the single-source method to obtain insoluble PB ($Fe_4[Fe(CN)_6]_3 \cdot xH_2O$), which is non-dispersible in water, in contrast to soluble PB ($KFe[Fe(CN)_6] \cdot xH_2O$), it has been synthesized using either hexacyanoferrate(II) or hexacyanoferrate(III) as the sole reactant. In the case of hexacyanoferrate(II), the current understanding of the reaction mechanism involves the acid-catalyzed hydrolysis of hexacyanoferrate(II), where the Fe^{3+} ions formed as a result of hydrolysis, and the reaction of this ion with intact hexacyanoferrate(II) complex ions, yielding insoluble PB.[13] Notably, in the case of hexacyanoferrate(III), understanding on the PB formation is largely limited.[11,13,14a] In the report by Domingo et al., the hydrolysis of $K_3Fe(CN)_6$ in perchloric acid ($HClO_4$) aqueous solution produces soluble PB ($KFe^{III}[Fe^{II}(CN)_6]$), with the mechanism involving the reaction between Fe^{3+}, generated by the hydrolysis of hexacyanoferrate(III), and intact hexacyanoferrate(II) reduced from hexacyanoferrate(III), resulting in PB.[14a] The report highlighted challenges encountered in interpreting the experimental data utilized to establish the paper's conclusions: Firstly, an inaccurate assumption was made regarding the mechanism of hexacyanoferrate(III) reduction to hexacyanoferrate(II) during acid-catalyzed hydrolysis. This

assumption attributed the reduction to the generation of cyanogen ($(CN)_2$), which had been reported to be produced *via* a solid-phase reaction unrelated to acid-catalyzed hydrolysis.[14b] Secondly, the conclusion drawn regarding the hydrolysis of hexacyanoferrate(III) to Fe^{3+} and subsequent reaction with unreacted hexacyanoferrate to form PB contradicts observations from UV-vis spectra, where a broad band (500-1000 nm) corresponding to the formation of PB could not be observed until the hydrolysis process was completed.

While PB and PBAs through the single-source method are commonly produced by the single-source or single-precursor method, to our knowledge, an exploration of the mechanistic details in this context has not been conducted. Elucidating these insights could propel the chemistry of PB forward and aid in developing a synthetic strategy for functional multimetallic PB.

In this study, we offer a *de novo* investigation into the mechanism and generation of reaction intermediates arising from the hydrolysis of the hexacyanoferrate(III) complex. The research aims to clarify these reaction intermediates through the utilization of UV-vis spectrophotometry, liquid chromatography-electrospray ionization mass spectrometry (LC-ESI-MS), and a specially designed hydrothermal reaction. Hence, the utilization of hexacyanoferrate(II/III) as the starting material for PB synthesis may not be imperative. Alternatively, a more cost-effective approach could involve employing potassium cyanide and iron ion species as the starting materials for synthesis.

EXPERIMENTAL

General

All the reagents were purchased from commercial sources and used without further purification. Deionized water was purified on a new P.Nix UP 900 water purification system (Human Corporation, South Korea). UV-vis spectra were obtained using an Agilent 8453 spectrophotometer (Santa Clara, CA, USA). Liquid chromatography-electrospray ionization-mass (LC-ESI-MS) spectra were obtained using an Agilent 6410B Triple Quad spectrometer (Santa Clara, CA, USA) in the Center for University-Wide Research Facilities, Jeonbuk National University. The diffraction patterns were collected from 10° to 90° at a scan rate of 5°/min (Cu Kα radiation (40 kV and 30 mA)) with a step size of 0.02° on a Rigaku MiniFlex diffractometer (Rigaku Corporation, Japan).

Kinetic Study on Hydrolysis of Hexacyanoferrate (III)

To investigate the kinetics of the hydrolysis of potassium hexacyanoferrate(III) in 1.0 M HCl solution at elevated temperatures, fresh stock solutions (5.0×10^{-2} M) were prepared in 1.0 M HCl aqueous solution before each time of the experiment. The stock solution was diluted to 6.0×10^{-4} M in 1.0 M HCl solution, and the diluted solutions were used to acquire time-based UV-vis spectra at three temperatures (70, 60, and 50 ℃). The reaction temperatures were limited within 50-70 ℃ because bubbles were generated in the solution at 80 ℃ and the reaction at 40 ℃ is too slow to observe the progress of the reaction in a practical time scale. The reaction concentration was maintained at 6.0×10^{-4} M, as indicated by the UV-vis spectra where the major peaks did not exceed an absorbance of 1. The quartz cuvette (1.0 cm) was immersed in a temperature-controlled water bath and used intermittently for the acquisition of UV-vis spectra.

The Devised Reaction

In a hydrothermal reaction conducted within a hydrothermal reactor (250 mL), vessel A containing ($FeCl_2 \cdot 4H_2O$: 50 mM; $FeCl_3 \cdot 6H_2O$: 50 mM) in 1.0 M HCl solution was immersed in vessel B containing potassium hexacyanoferrate(III) (100 mM) in 1.0 M HCl aqueous solution. Notably, the two vessels were positioned to avoid direct contact with each other, and vessel A remained open to facilitate reaction with gaseous HCN. The reaction temperature was controlled in an electric heating oven at 120 ℃ and maintained at the temperature for 2 days. After completion, two separate solutions were isolated to confirm the reaction products in each vessel. In vessel A, no PB was observed, therefore, the solution was diluted to 6.0×10^{-4} M solution to acquire a UV-vis spectrum. In vessel B, a deep blue precipitate was isolated from the solution and the precipitate was washed with water and ethanol several times in a centrifuge and dried in an oven overnight.

LC-ESI-MS Experiments

The liquid chromatography-electrospray ionization-mass (LC-ESI-MS) spectra were obtained using an Agilent 6410B Triple Quad spectrometer (Santa Clara, CA, USA), in either positive-ion mode or negative-ion mode, by introducing the sample in 1.0 M HCl aqueous solution obtained from our experiments with a buffer consisting of two buffers (A:B = 95:5 v/v(%), buffer A: 0.1% formic acid in deionized water, buffer B: 0.1% formic acid in acetonitrile). The samples were continuously injected into the spectrometer by a syringe pump at a flow rate of 0.5 mL/min. Instrumental parameters include a sprayer voltage of 3.0 kV optimized to enhance the signal-to-noise ratio of the spec-

tra and a capillary temperature of 300 ℃ to facilitate the evaporation of the solvent containing water and desolvation of aquated iron ions without affecting the results. The sample duration in the instrument was adjusted to 0.2 seconds, a duration deemed sufficient to minimize alterations in the oxidation states of metal ions.

RESULTS AND DISCUSSION

Hexacyanoferrate(III), characterized as a strong-field d^5 and inert complex ion, exhibits high resistance to hydrolysis, with a stability constant ($\log K_s$) known to be 43.9.[15] The successive pK_as of $H_3Fe(CN)_6$ were determined as pK_1 = -6.25 ± 0.10, pK_2 = -3.24 ± 0.03, and pK_3 = -0.60 ± 0.02,[14] indicating the presence of monoprotonated ($HFe(CN)_6^{2-}$) and fully deprotonated ($Fe(CN)_6^{3-}$) forms in a 1.0 M aqueous HCl solution. Hereafter, the reactant will be referred to as $Fe(CN)_6^{3-}$.

Observing a series of absorption bands of $Fe(CN)_6^{3-}$ at 260, 285, 320, and 420 nm, corresponding to *d-d* transition bands ($^2T_{1g} \rightarrow {}^2E_{1g}$, $^2T_{2u} \rightarrow {}^2T_{2g}$, $^2T_{2g} \rightarrow {}^2A_{1g}$, and $^2T_{1g} \rightarrow {}^2T_{2g}$ transitions),[16] the molar extinction coefficient (ε) was determined to be 1045 ± 10 L·mol^{-1}·cm^{-1} at 420 nm (*Fig.* S1). UV-vis absorption spectrophotometric experiments conducted at 70, 60, and 50 ℃ (reactions **1**, **2**, and **3**) revealed first-order kinetics at each temperature. *Fig.* 1 illustrates the UV-vis spectra of hexacyanoferrate at 70 ℃ over time (reaction **1**), where the band at 420 nm diminishes, following first-order kinetics. The first-order kinetics means the substitution reaction may undergo a dissociative mechanism commonly found in 6-coordinate complexes. However, the pseudo-first-order rate constant due to a large excess of H_3O^+ and Cl^- compared to $Fe(CN)_6^{3-}$ could not disregarded. *Fig.* S2 depicts a linear relationship in the graph of ln[A]$_t$ vs. t, allowing the estimation of the observed rate constant (k_{obs}) as 1.21 × 10^{-4} (± 0.02 × 10^{-4}) s^{-1}. The experiments at 60 ℃ (reaction **2**) and 50 ℃ (reaction **3**) yield rate constants of 3.77 × 10^{-5} (± 0.10 × 10^{-5}) s^{-1} and 9.19 × 10^{-6} (± 0.49 × 10^{-6}) s^{-1}, respectively (*Fig.* S3 and S4). Utilizing these rate constants, the preliminary activation energy (E_a) and pre-exponential factor (A) were calculated as 119 kJ mol^{-1} and 2.15 × 10^{14} s^{-1}, respectively, using the *Arrhenius* equation (*Fig.* S5).

Interestingly, the UV-vis spectrum in *Fig.* 1 reveals an isosbestic point around 389 nm. An isosbestic point indicates that only two species that vary in concentration contribute to the absorption around the point. Therefore, one species exhibiting decreasing absorbance corresponds to hexacyanoferrate(III), while the other species could potentially represent a single hydrolyzed product. We hypothesized regarding the peak exhibiting growth and peak-shifting (320 nm~332 nm), suggesting the presence of either partially or fully hydrolyzed species. However, the observed spectrum pattern diverges significantly from that of partially hydrolyzed species, such as the $Fe(CN)_5(H_2O)^{2-}$ species generated by the irradiation of 366 nm light.[18] Instead, it could be assigned as the aquated iron species because the region is quite close to the absorption pattern of Fe^{3+} ions (λ_{max} = 335 nm), which are presumably composed of various aquatic forms such as $Fe(H_2O)_6^{3+}$, $Fe(H_2O)_5(OH)^{2+}$, $Fe(H_2O)_4(OH)_2^+$, and chlorinated forms such as $[Fe(H_2O)_5Cl]^{2+}$, *trans*-$[Fe(H_2O)_4Cl_2]^+$, $[Fe(H_2O)_3Cl_3]$ and $[FeCl_4]^-$ in the solution containing complexing Cl^- ion.[18] Notably, the UV-vis spectrum in *Fig.* 2 for reaction **2** after 540 min, which is

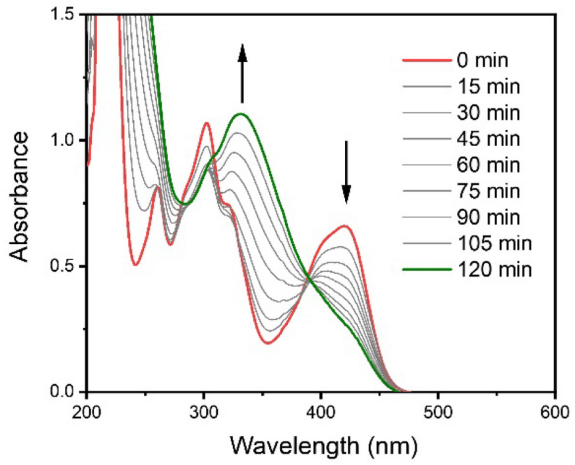

***Figure* 1.** Time-based UV-vis spectra of potassium hexacyanoferrate(III) in 1.0 M HCl solution at 70 ℃ (reaction **1**).

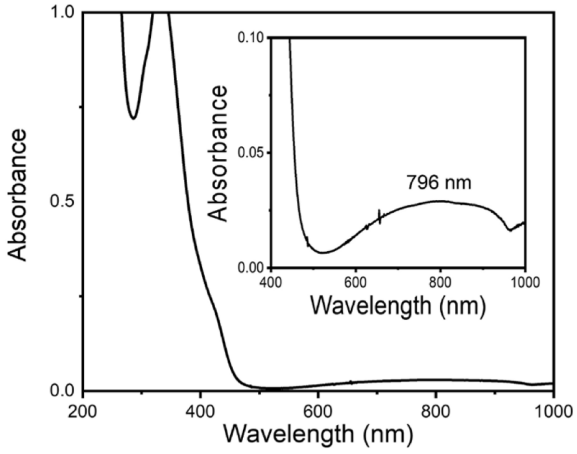

***Figure* 2.** UV-vis spectrum of the hydrolysis of potassium hexacyanoferrate(III) in 1.0 M HCl aqueous solution at 60 ℃ after 540 min (reaction **2**). Inset: A magnified view of the spectrum.

sufficient time to complete the hydrolysis, reveals a broad band from 500-1000 nm, indicative of PB suspension dispersed in the solution.[19] This observation signifies the complete hydrolysis of hexacyanoferrate(III) preceding the formation of PB.

To probe the reaction intermediates further, liquid chromatography-electrospray ionization-mass spectrometric (LC-ESI-MS) experiments were conducted following reaction **1** after 2 h. Initially, a positive-ion mode LC-ESI-MS experiment was performed, but *Fig*. S6 demonstrates that a spectrum with a sufficiently high signal-to-noise ratio for accurate species assignment could not be acquired. Consequently, negative-ion mode LC-ESI-MS experiments were undertaken to detect metal ion species. The resulting spectrum distinctly reveals the predominant presence of $Fe^{II}Cl_3^-$ (*m/z* = 162.7) and $Fe^{III}Cl_4^-$ (*m/z* = 197.5) species, with an intensity ratio of 0.74:1, as depicted in *Fig*. 3. Notably, chlorinated anions and the reduced chlorinated species $Fe^{II}Cl_3^-$ are observed. In a negative-ion mode LC-ESI-MS environment, Fe^{3+} ions are deemed prone to reduction to Fe^{2+}.[20] As a control experiment, the negative-ion mode LC-ESI-MS spectrum of $FeCl_3 \cdot 6H_2O$ (6.0×10^{-4} M) dissolved in 1.0 M HCl aqueous solution was examined. In this control, $Fe^{II}Cl_3^-$ is detected with significantly lower intensity compared to $Fe^{III}Cl_4^-$, with an intensity ratio of 0.06:1 (*Fig*. S7). This observation leads to the conclusion that the $Fe^{II}Cl_3^-$ species likely stems from the hydrolysis of hexacyanoferrate(III) during the reaction with high probability. Intriguingly, no peaks corresponding to hexacyanoferrate(III) and other partially decyanated iron species were detected, aligning with the UV-vis kinetic study, wherein hexacyanoferrate(III) is solely converted to aqueous iron species (*Fig*. 3). Moreover, the LC-ESI-MS spectrum obtained from a freshly prepared 1.0 M HCl solution of $K_3Fe(CN)_6$ (6.0×10^{-4} M) to monitor the metallic species appearing at the early stage of the reaction, illustrates the presence of $K_2Fe^{III}(CN)_6^-$ (*m/z* = 289.9), $K_2Fe^{II}(CN)_5^-$ (*m/z* = 263.9), $KH_2Fe^{II}(CN)_6^-$ (*m/z* = 252.9), $KFe^{II}(CN)_4^-$ (*m/z* = 198.6), and $Fe^{II}(CN)_3^-$ (*m/z* = 133.9) in *Fig*. 4. This observation underscores that the LC-ESI-MS spectrum of a freshly prepared $Fe(CN)_6^{3-}$ solution not only markedly differs from that of the spectra subsequent to reaction **1**, which exclusively generated chlorinated iron species, but also elucidates the non-innocent nature of the cyano ligand, which is aligning with the formation of Fe(II) species as the product of hydrolysis during the reaction (*Fig*. 4).[21] The detection of reduced decynated species using hexacyanoferrate(III) is commonly observed even in a neutral pH solution.[22] Consequently, the commonly conjectured mechanism of the single-source method, involving the combination of Fe^{3+} ions generated by the hydrolysis of hexacyanoferrate(III), and intact hexacyanoferrate(II) reduced from hexacyanoferrate(III) to produce PB ($Fe_4[Fe(CN)_6]_3 \cdot xH_2O$), may need reconsideration.

The following experiment focuses on the detection of hydrocyanic acid (HCN) as an intermediate species. The presence of HCN is attributed to the fact that the cyanide ion (CN^-) is the conjugate base of HCN with a pK_a of 9.2. HCN can either be dissolved in the reaction medium or be in a gaseous state outside the medium due to its lower density than air and limited solubility, dictated by a low Henry's law constant (k_H) at elevated temperatures, even though

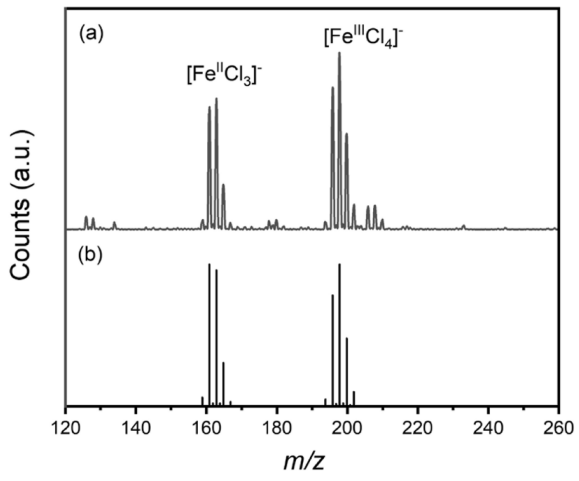

***Figure* 3.** (a) A negative-ion mode LC-ESI-MS spectrum after reaction **1** at 70 ℃, and (b) the calculated mass spectrum of $FeCl_3^-$ and $FeCl_4^-$.

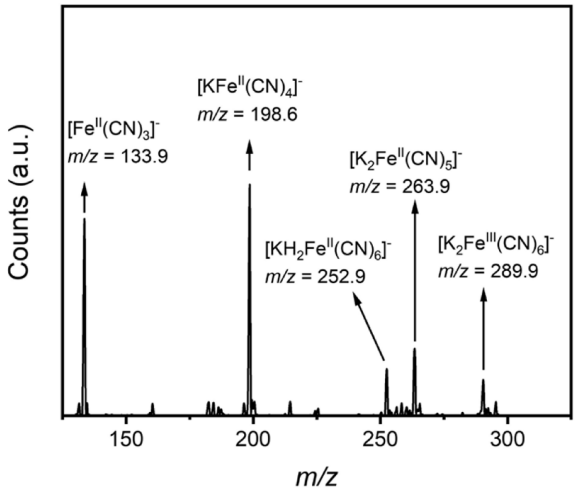

***Figure* 4.** A negative-ion mode LC-ESI-MS spectrum of a freshly prepared aqueous 1.0 M HCl solution of hexacyanoferrate(III) (6.0×10^{-4} M).

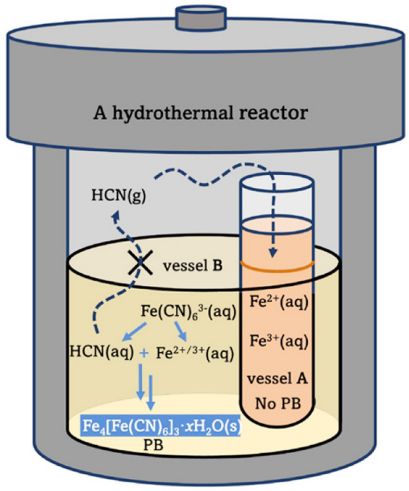

***Scheme* 1.** Schematic diagram of the devise experiment.

the constant measured in buffered water at pH 9.0.[23] The latter implies that the solubility of HCN gas in water decreases with increasing water temperature, consistent with common gases. On a contrasting note, the high gas-phase proton affinity (PA) of HCN (712 kJ/mol) suggests slightly higher basicity compared to water (691.1 kJ/mol).[24] A direct correlation with solution-phase basicity may not be evident in gas-phase basicity. However, the potential of HCN to act as a base in acidic conditions cannot be disregarded. Should the formation of $HCNH^+$ take place, it would persist as an ion within the aqueous phase. To investigate the presence of HCN in the aqueous phase, we devised an experiment utilizing a hydrothermal reactor, as shown in *Scheme* 1. In this setup, a test tube (vessel **A**) containing dissolved Fe^{2+} and Fe^{3+} (50 mM and 50 mM each) in 1.0 M HCl solution is immersed into another vessel (vessel **B**) containing potassium hexacyanoferrate(III) (100 mM) solution in a hydrothermal reactor and the reaction was conducted at 120 ℃ for 2 d. In this experimental scenario, if HCN were to escape from the solution in vessel **B**, it would react with the solution in vessel **A**, leading to the formation of PB. However, upon completion of the reaction, no PB was observed in vessel **A**, as depicted in the UV-vis spectrum of the solution in *Fig.* 5a, in contrast to the evident PB formation in vessel **B**. The powder XRD pattern of the solid product isolated from vessel **B**, as shown in *Fig*. 5b, aligns with the reported PB pattern (JCPDS No.: 01-073-0689).[25] Our interpretation suggests that HCN resides in the aqueous phase rather than escaping to the gas phase. Therefore, $Fe^{2+/3+}$ ions are anticipated to react with HCN, leading to the formation of PB through the following overall reactions:

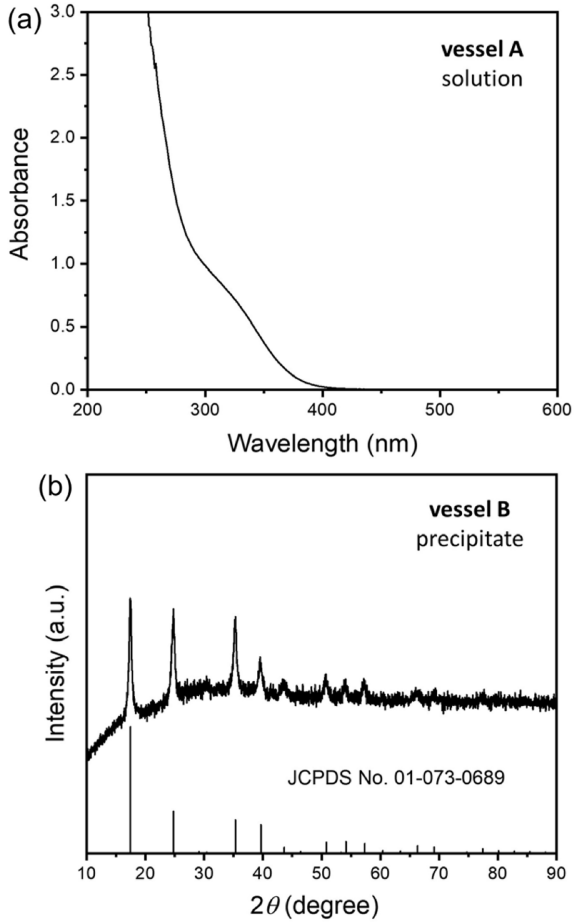

***Figure* 5.** (a) UV-vis spectrum of a diluted solution (6×10^{-4} M) of vessel **A**, and (b) powder X-ray diffraction (XRD) pattern of the product in vessel **B** (JCPDS No. 01-073-0689), after the devised reaction, as shown in *Scheme* 1.

$$Fe(CN)_6^{3-}(aq) + 6\ H_3O^+(aq) \rightarrow Fe(H_2O)_6^{2+/3+}(aq) + 6\ HCN(aq) \quad (1)$$

$$HCN(aq) \rightarrow H^+(aq) + CN^-(aq)\ pK_a = 9.2 \quad (2)$$

$$7\ Fe(H_2O)_6^{2+/3+}(aq) + 18\ CN^-(aq) \rightarrow Fe_4[Fe(CN)_6]_3 \cdot xH_2O(aq) \quad (3)$$

In conjunction with the acidic conditions, the acid dissociation constant (K_a) of HCN suggests that the significantly lower concentration of CN^- compared to HCN may retard PB formation. Therefore, CN^- acts as the limiting reagent for the product, which helps form PB with a $Fe^{2+/3+}$:CN^- molar ratio of 1:2.57 rather than $Fe(CN)_6^{3-/4-}$ with the molar ratio of 1:6. Considering the high lattice energy, a more thermodynamically stable PB is ultimately generated.[26] Therefore, we propose a sequential mechanism in that the $Fe(CN)_6^{3-}$ is hydrolyzed to yield aquated or chlorinated $Fe^{2+/3+}$ ions and HCN, which subsequently engage with each other, leading to the formation of PB.

CONCLUSION

Collectively, our discoveries indicate that the acid-catalyzed hydrolysis of $Fe(CN)_6^{3-}$ adheres to a "sequential mechanism", which is supported by the identification of an isosbestic point in the UV-vis spectra, the negative-ion mode LC-ESI-MS, and the devised experiment. Despite the necessity for further exploration into the generation of the reduced iron form, Fe^{2+}, after the hydrolysis of hexacyanoferrate(III), and the detailed formation mechanism of PB from iron species and HCN, it is crucial to note that this mechanism deviates from the conventional assumptions associated with the single-source method employing hexacyanoferrate(II/III). This investigation not only enriches our understanding of PB formation in the single-source method but also contributes to the abandonment of single-source or single-precursor methods that utilize hexacyanoferrate(II/III) as the single starting material for PB synthesis. Alternatively, a more cost-effective approach could involve employing potassium cyanide and iron ion species as the starting materials for the synthesis. Moreover, the facile synthesis of multi-metallic PB could be achieved by incorporating diverse metal ions alongside potassium cyanide. However, further investigation is needed to understand the formation of Fe^{2+} ions during hydrolysis. An alternative synthetic approach for nanocrystalline PB synthesis also requires consideration. Our current efforts are focused on exploring the potential in this area.

Acknowledgments. Publication cost of this paper was supported by the Korean Chemical Society.

Supporting Information. The UV-vis spectra for the determination of the molar extinction coefficient, the kinetic study, LC-ESI-MS data are available online.

REFERENCES

1. (a) Kraft, A. *ChemTexts* **2018**, *4*, 16. (b) Ludi, A. *J. Chem. Educ.* **1981**, *58*, 1013.
2. (a) Ferrer-Vilanova, A.; Alonso, Y.; Ezenarro, J. J.; Santiago, S.; Muñoz-Berbel, X.; Guirado, G. *ACS Omega* **2021**, *6*, 30989. (b) Aller-Pellitero, M.; Fremeau, J.; Villa, R.; Guirado, G.; Lakard, B.; Hihn, J.-Y.; del Campo, F. *J. Sens. Actuators B Chem.* **2019**, *290*, 591.
3. (a) Aaseth, J.; Nurchi, V. M.; Andersen, O. Biomolecules **2019**, *9*, 856. (b) Hoffman, R. S. *Toxicol. Rev.* **2003**, *22*, 29.
4. (a) Nakotte, H.; Shrestha, M.; Adak, S.; Boergert, M.; Zapf, V. S.; Harrison, N.; King, G.; Daemen, L. L. *J. Sci. Adv. Mater. Devices* **2016**, *1*, 113. (b) Ferlay, S.; Mallah, T.; Ouahès, R.; Veillet, P.; Verdaguer, M. *Nature* **1995**, *378*, 701. (c) Huang, Y.; Ren, S. *Appl. Mater. Today* **2021**, *22*, 100886.
5. (a) Thallapally, P. K.; Motkuri, R. K.; Fernandez, C. A.; McGrail, B. P.; Behrooz, G. S. *Inorg. Chem.* **2010**, *49*, 4909. (b) Karadas, F.; El-Faki, H.; Deniz, E.; Yavuz, C. T.; Aparicio, S.; Atilhan, M. *Microporous Mesoporous Mater.* **2012**, *162*, 91. (c) Motkuri, R. K.; Thallapally, P. K.; McGrail, B. P.; Ghorishi, S. B. *CrystEngComm* **2010**, *12*, 4003.
6. (a) Kaye, S. S.; Long, J. R. *J. Am. Chem. Soc.* **2005**, *127*, 6506. (b) Krap, C. P.; Balmaseda, J.; del Castillo, L. F.; Zamora, B.; Reguera, E. *Energy Fuels* **2010**, *24*, 581.
7. Sitnikova, N. A.; Komkova, M. A.; Khomyakova, I. V.; Karyakina, E. E.; Karyakin, A. A. *Anal. Chem.* **2014**, *86*, 4131.
8. (a) Zhang, Z.; Avdeev, M.; Chen, H. *Nat. Commun.* **2022**, *13*, 7790. (b) Nie, P.; Shen, L.; Luo, H.; Ding, B.; Xu, G.; Wang, J.; Zhang, X. *J. Mater. Chem. A* **2014**, *2*, 5852. (c) Wang, W.; Gang, Y.; Hu, Z.; Yan, Z.; Li, W.; Li, Y.; Gu, Q.-F.; Wang, Z.; Chou, S.-L.; Liu, H.-K.; Dou, S.-X. *Nat. Commun.* **2020**, *11*, 980. (d) Qian, J.; Wu, C.; Cao, Y.; Ma, Z.; Huang, Y.; Ai, X.; Yang, H. *Adv. Energy Mater.* **2018**, 1702619. (e) Niu, B.; Jiang, W.; Jiang, B.; Lv, M.; Wang, S.; Wang, W. *Nat. Commun.* **2022**, *13*, 2316.
9. (a) Vyboishchik, A. V.; Popov, M. Y. *IOP Conf. Ser.: Mater. Sci. Eng.* **2020**, *962*, 022035. (b) Ludi, A.; Guedel, H. U.; Ruegg, M. *Inorg. Chem.* **1970**, *9*, 2224. (c) Shriver, D. F.; Shriver, S. A.; Anderson, S. E. *Inorg. Chem.* **1965**, *4*, 725. (d) Yan, N.; Hu, L.; Li, Y.; Wang, Y.; Zhong, H.; Hu, X.; Kong, X.; Chen, Q. *J. Phys. Chem. C* **2012**, *116*, 7227.
10. (a) Risset, O. N.; Knowles, E. S.; Ma, S.; Meisel, M. W.; Talham, D. R. *Chem. Mater.* **2013**, *25*, 42. (b) Guo, S.; Wang, H.; Tricard, S.; Zheng, P.; Sun, A.; Fang, J.; Zhao, J. *Ind. Eng. Chem. Res.* **2020**, *59*, 13831. (c) Gao, Y.; Liu, H.; Zheng, Z.; Luan, X.; Xue, Y.; Li, Y. *NPG Asia Mater.* **2023**, *15*, 12.
11. (a) Zhang, L.; Wu, H. B.; Madhavi, S.; Hng, H. H.; Lou, X. W. *J. Am. Chem. Soc.* **2012**, *134*, 17388. (b) Wu, X.; Cao, M.; Hu, C.; He, X. *Cryst. Growth Des.* **2006**, *6*, 26. (c) Ding, Y.; Hu, Y.-L.; Gu, G.; Xia, X.-H. *J. Phys. Chem. C* **2009**, *113*, 14838. (d) Hu, M.; Belik, A. A.; Imura, M.; Yamauchi, Y. *J. Am. Chem. Soc.* **2013**, *135*, 384. (e) Hu, M.; Furukawa, S.; Ohtani, R.; Sukegawa, H.; Nemoto, Y.; Reboul, J.; Kitagawa, S.; Yamauchi, Y. *Angew. Chem. Int. Ed.* **2012**, *51*, 984. (f) Shen, X.; Wu, S.; Liu, Y.; Wang, K.; Xu, Z.; Liu, W. *J. Colloid Interface Sci.* **2009**, *329*, 188. (g) Kang, S.; Im, S.; Jeon, Y. *Bull. Kor. Chem. Soc.* **2015**, *36*, 2387.
12. (a) Jeon, Y.; Choi, K.; Im, S. *Bull. Kor. Chem. Soc.* **2015**, *36*, 2966. (b) Jeon, Y.; Choi, K.; Im, S. *Bull. Kor. Chem. Soc.* **2015**, *36*, 2970.
13. Jia, Z.; Sun, G. *Colloids Surf. A Physicochem. Eng. Asp.* **2007**, *302*, 326.
14. (a) Domingo, P. L.; Garcia, B.; Leal, J. M. *Can. J. Chem.* **1990**, *68*, 228. (b) P. G. Sim, E. Whalley *J. Phys. Chem.* **1987**, *91*, 1877.

15. Beck, M. T. *Pure Appl. Chem.* **1987**, *59*, 1703.
16. Ayers, J. B.; Waggoner, W. H. *J. Inorg. Nucl. Chem.* **1971**, *33*, 721.
17. Fuller, M. W.; Lebrocq, K. M. F.; Leslie, E.; Wilson, I. R. *Aust. J. Chem*. **1986**, *39*, 1411.
18. (a) Torras, M.; Moya, C.; Pasquevich, G. A.; Roig, A. *Microchim. Acta* **2020**, *187*, 488. (b) Abderrazak, H.; Dachraoui, M.; Lendl, B. *Analyst* **2000**, *125*, 1211. (c) Ng, K. C.; Adel, T.; Lao, K. U.; Varmecky, M. G.; Liu, Z.; Arrad, M.; Allen, H. C. *J. Phys. Chem. C* **2022**, *126*, 15386.
19. Pandurangappa, M.; Samrat, D. *Anal. Sci.* **2010**, *26*, 83.
20. Mollah, S.; Pris, A. D.; Johnson, S. K.; Gwizdala III, A. B.; Houk, R. S. *Anal. Chem.* **2000**, *72*, 985.
21. Jach, F.; Block, T.; Prots, Y.; Schmidt, M.; Bobnar, M.; Pöttgen, R.; Ruck, M.; Höhn, P. *Dalton Trans.* **2022**, *51*, 7811.
22. Moraes, M. C. B.; Brito Neto, J. G. A.; do Lago, C. L. *Int. J. Mass Spectrom.* **2000**, *198*, 121.
23. Ma, J.; Dasgupta, P.; Blackledge, W.; Boss, G. S. *Environ. Sci. Technol.* **2010**, *44*, 3028.
24. (a) Walder, R.; Franklin, J. L. *Inter. J. Mass Spectrom. Ion Phys.* **1980**, *36*, 85. (b) Hunter, E. P. L.; Lias, S. G. *J. Phys. Chem. Ref. Data* **1998**, *27*, 413.
25. Herren, F.; Fischer, P.; Ludi, A.; Haelg, W. *Inorg. Chem.* **1980**, *19*, *4*, 956.
26. Rosseinsky, D. R.; Glasser, L.; Jenkins, H. D. B. *J. Am. Chem. Soc.* **2004**, *126*, 10472.